Sniffer Worm, C. elegans, as a Toxicity Evaluation Model Organism with Sensing and Locomotion Abilities

Jun Sung Kim
Korea Advanced Institute of Science and Technology
Sang-Kyu Park
Soonchunhyang University
Haeshin Lee (haeshin@kaist.ac.kr)
Korea Advanced Institute of Science and Technology

Research Article

Keywords: probability, three-dimensional (3D) printing, nozzle temperature, toxic component, animal model system

Posted Date: December 28th, 2020

DOI: https://doi.org/10.21203/rs.3.rs-128170/v1

Abstract

The probability of objects fabricated by three-dimensional (3D) printing exhibiting local defects is higher than that detected in products of conventional casting-based manufacturing. Multistep layer-by-layer procedures in additive manufacturing are the main reason. Light intensity and/or penetration depth, inhomogeneity of components, and variations in nozzle temperature are factors that create local defects. Defect regions are sources of toxic component release, but methods to identify them in printed materials have not been reported. Existing assays for evaluating material toxicity are based on extraction, and these toxicological assays use living creatures to passively detect harmful agents in extracted solutions. Thus, the development of an active system for identifying sites of toxicity sources is a critical and urgent issue in 3D printing technologies. Herein, we introduce an animal model system, *C. elegans*, for toxicity evaluation. *C. elegans* crawls toward safe regions but avoids toxically dangerous areas. The 'sensing' and 'locomotion' abilities of *C. elegans* are unparalleled among existing underwater and animal models, providing immediate indications to help find toxicity source sites.

Introduction

One critical and unavoidable step in developing new materials for biomedical applications is the toxicological evaluation of newly developed materials.[1] Living organisms must be chosen when evaluating material toxicity. Early studies in toxicological tests utilized plant species such as *Lemna gibba*.[2] This plant is small in size, easily grown, and short in life cycle.[3,4] An advantage of this approach is that growth inhibition by any toxic components can be easily observed. However, the results of *Lemna gibba* growth inhibition are not directly related to toxicological effects on humans.

Due to the aforementioned limitations related to correlation with human toxicity levels, later studies have introduced animal models. Two categories have been developed. One involves underwater organisms, such as *Daphnia*[5,6] or *Danio rerio* (zebrafish),[7,8] and the other is based on terrestrial animals, for instance, a rat or a mouse.[9] Toxicological outcomes observed in underwater animals are expressed by one or more factors via the following: acute immobilization, mobility, survival, developmental disorder, and/or embryo hatching.[6] However, the results obtained in underwater environments are very different from those obtained in ambient conditions. Thus, terrestrial animal models have become popular. Rats and mice have been dominantly chosen as animal models recently because they are small and inexpensive compared to other mammals and produce many descendants. However, strict and wide-ranging ethical regulations have recently become a major obstacle to the use of model systems.[10] For this reason, organ-on-a-chip or related technologies have been introduced,[11] and cosmetic science has just begun to find an alternative method to test the toxicity of newly introduced components.

The aforementioned challenges in current model systems motivate researchers to develop a new convenient and effective way to address this ethical issue. Importantly, additive manufacturing technologies known as 3D printing also require a novel toxicity evaluation system.[12] Compared to those

manufactured by a conventional casting-based method, objects prepared by 3D printers intrinsically present many defective regions. When building up an object, Additive layer-by-layer deposition processes essentially go through many repeated steps during which unavoidable defects are generated. For stereolithography (SLA) methods, light intensity and/or penetration depth, inhomogeneity in polymers concentrations, and dispersion of components can slightly vary.[13] For fused deposition modeling (FDM), variations in nozzle temperature in systems are a factor that create local defects when printing an object.[14] As 3D printing techniques are suitable for small-quantity prototype production, each product exhibits varied sites of defects that result in a different level of toxicity.

Therefore, the development of a new animal model that detects product-to-product variations in toxicity sources is necessary. Unfortunately, the aforementioned plant and animal models cannot satisfy this need (Table 1). In the case of plant models, the living creature has no locomotive function to identify sites of toxicological sources in printed materials. The underwater toxicity evaluation system, zebrafish, has a locomotive function, but leached toxic compounds are diffused in water. Thus, zebrafish are not a suitable model system for identifying the toxicity sources in printed materials. Foreign body reactions to implanted materials in mice and rats also make it difficult to identify toxicity sources.

Table 1
Typical model organism list and their chemical detection ability and locomotion

	Model system	Sensing	Locomotion	Remarks
Animal	Zebrafish	O	O	Lives underwater
	Daphnia sp.	O	O	
	Rodent(rat, mouse)	O	O	Ethical issues
	C. elegans	O	O	
Plant	*Lemna gibba*	O	X	Does not move
	Arabidopsis thaliana	O	X	
Others	Mammalian cell lines	O	X	Cannot move in a reasonable time
	Fungi(*Saccharomyces cerevisiae*)	O	X	
	Bacteria(*Escherichia coli*)	O	X	

For the aforementioned reasons, the combination of sensing and locomotion is an important factor in the development of a new toxicity model. Here, we propose *Caenorhabditis elegans* (*C. elegans*) as a model that can detect both overall toxicity and toxic sites of printed materials. The reason for choosing *C. elegans* is that it essentially exhibits chemotactic behavior.[15] The crawling behavior of *C. elegans* provides phenotypic indications for detecting sources of toxicity origins in a test material. In addition, the lifespan of *C. elegans* is from two to four weeks, which is suitable for a model system.[16] *C. elegans* is one

of a few creatures where all its genome sequences are known.[17] The body length of the adult worm is approximately 1 mm, and all differentiation pathways of 959 cells in total from a single germinal cell are reported, which also makes *C. elegans* suitable for evaluating toxicity effects.[18] This attractive animal has already been studied in various fields, such as aging, new drug development, and neurobiology.[19–23] However, considerations and attempts to utilize *C. elegans* as an 'active' toxicological model with sensing and locomotion abilities have never been studied.

Results

♦ Effect of 3D printed blocks extracted LB on lifespan

We hypothesized the following. First, Luria-Bertani broth (LB) media were prepared because the energy source of *C. elegans* is bacteria, for which *Escherichia coli* (OP50) has been widely used. Second, any toxic compounds released from 3D-printed cuboids ($1 \times 1 \times 0.1$ cm^3, 80 units incubation in 400 mL of LB, Fig. 1A) might be adsorbed during *E. coli* growth. Third, the *C. elegans* eating the contaminated *E. coli* might exhibit a reduced lifespan. Figure 1B clearly shows that the maximal lifespan of *C. elegans* living with the supplement of *E. coli*, which is grown in LB containing toxic compounds extracted from the cuboids, was decreased from 24 (black) to 20 (red) days. A control experiment used LB media without toxic compound extraction from the cuboids. Importantly, the mean lifespan, defined by 50% survival of *C. elegans*, was 15 days for the control, which was decreased to approximately 13 days for the treatment group (dotted lines, Fig. 1B). Three independent experiments were performed, and all detailed lifespan parameters are listed in Table 2. In conclusion, the decrease in longevity caused by the toxic compounds released from the 3D-printed cuboid was 15.8% ($p < 0.05$).

Table 2
Reduction in the lifespan of *C. elegans* by 3D-printed block extract

		Mean Lifespan (days) [a]	Max. Lifespan (days) [b]	*p*-value [c]	% decreased [d]
1st	Control	16.68	24	< 0.001	20.83
	Extracts	13.20	20		
2nd	Control	14.95	23	< 0.05	13.50
	Extracts	12.93	19		
3rd	Control	14.88	22	< 0.05	12.48
	Extracts	13.02	19		
Average	Control	15.50	23	< 0.05	15.80
	Extracts	13.05	19.33		

[a] Mean lifespan is the day when 50% of worms survived. [b] Max. lifespan is the greatest age reached by the last surviving worm. [c] p-value was calculated using the log-rank test by comparing the survival of the control group and the group exposed to 3D-printed block extract (marked as "Extracts" in the table). [d] % effects were calculated by (C-E)/C*100, where E is the mean lifespan of *C. elegans* treated with extracts and C is the mean lifespan of the control *C. elegans*.

♦ Relative expression levels of a stress-response gene

As we observed a lifespan reduction of *C. elegans* exposed to the extract of a 3D-printed cuboid, we assumed that there might be a gene indicator to provide further evidence at the molecular level. We chose *hsp-16.2* and *sod-3*. *hsp-16.2* is a stress-responsive reporter gene that predicts longevity in *C. elegans*.[22] The expression level of *hsp-16.2* is correlated with increased resistance to heat-shock stress and increased lifespan in *C. elegans*.[24] *sod-3* is an antioxidant gene involved in the cellular enzymatic defense system against reactive oxygen species.[25] The worms were exposed to 3D-printed cuboids for 2 days after the adult stage. We observed a significant downregulation of *hsp-16.2* in worms treated with 3D-printed cuboid extract (Fig. 1C upper panels and 1D left bars). Green fluorescent images were obtained because of the expression of the fusion protein HSP-16.2-GFP (Fig. 1C). Qualitative analysis shows that the overall level of green fluorescence was considerably decreased. In addition, quantitative analysis (n = 20 for each group) was also performed. The relative expression level of *hsp-16.2* decreased to 52.96 ± 6.37% for the *C. elegans* supplemented with the 3D-printed cuboid extract (Fig. 1D, left bars). A similar result was obtained for SOD-3-GFP expression (74.92 ± 6.34% for the 3D cuboid extract group) (Fig. 1C lower panels and 1D right bars). Therefore, the nematodes exposed to 3D-printed cuboid extract are thought to be less able to resist stress.

♦ Toxic substance effects on C. elegans fertility

We assume that the toxic substances released from the cuboids might affect the fertility of *C. elegans*. In general, approximately 300 eggs are hatched in the entire lifetime of a healthy nematode.[26] Thus, tens of eggs can be found in a plate even after one day of culture of a single *C. elegans* organism.[27] Negative effects on fertility can be observed for *C. elegans* organisms that are exposed to the toxic substances released into LB. We designed an interesting experiment to observe these toxic effects influencing the fertility of *C. elegans*. First, all *C. elegans* nematodes were synchronized in their age. Second, a single worm was transferred to one plate of nematode growth medium (NGM). Third, incubation at 20 ℃ was carried out for 24 hrs, and then the incubated *C. elegans* was transferred again to a new NGM plate. Importantly, the empty plate incubated for 24 hrs (Fig. 2A) was not discarded but rather placed in the same incubator (20 ℃). The reason is to observe the *C. elegans* offspring hatched from the remaining eggs (# marked plates in Fig. 2A). The transfer process of the single *C. elegans* worm was continued for 6 days until no hatched *C. elegans* offspring were found. We checked the number of offspring at two days after each transfer. Figure 2B shows the mean number of progeny hatched by 5 individual worms on each day. The overall trend regarding the number of offspring per day showed a decreased number of offspring from the *C. elegans* exposed to the toxic compound LB extract: 8 at 2 days, 34 at 3 days, 11 at 4 days, and 4 at 5 days. Asterisks indicate p-values less than 0.05 compared with the control.

♦ C. elegans motility test: effect of using 3D-printed cuboid-extracted water

For the previous LB case, we observed overall negative toxicity results regarding lifespan, stress-response genes, and fertility. These results are due to the contaminated *E. coli* bacteria that were prepared in media into which toxic substances had been released. A different type of extraction is replacing LB media with distilled water (Fig. 2C). This simple replacement results in a large difference in the toxicity mode of action. The adverse substances are not in the food (i.e., *E. coli*) but rather in water. As *C. elegans* is able to swim by bending its body in an aqueous solution, we hypothesized that the speed of bending mobility could be affected. Approximately ten nematodes (age synchronized as 3 days) were transferred to either regular NGM or contaminated NGM by cuboid-extracted water (2 days). Finally, the worms on NGM were washed with M9 buffer and transferred to a 96-well plate to observe the bending speed of each group of *C. elegans*. We counted the number of body bends for 1 minute. Figure 2E shows time-lapse photo arrays representing body bending. For a healthy *C. elegans* worm, it takes approximately 1.6 sec to bend its body to an opposite position (upper photos). However, we observed that twice the time was required for the same bending motion in the case of the exposed worms (lower photos). Quantitative analysis showed that the unexposed worms (control) bent 53.2 times per minute (n = 6), which was decreased to 24 bends per minute for the exposed *C. elegans* (n = 6) (Fig. 2D). Thus, the overall motility test clearly demonstrated the adverse motility effect of the use of contaminated water produced from cuboid extraction.

♦ Identification of toxicity origin by X-ray photoelectron spectroscopy (XPS)

In general, biological toxicity when using photocurable resins is largely dependent on the photoinitiators.[28] However, knowledge of the resin composition used in this study is quite limited due to the company's proprietary right. Nevertheless, it is expected that the resin contains at least a certain amount of photoinitiators. We thought that unreacted photoinitiators would remain inside of the 3D-printed products until they eventually leached out and adversely affected the health of *C. elegans*. In Fig. 3A, the chemical structures of widely used UV-curable photoinitiators are presented: 2-benzyl-2-(dimethylamino)-4'-morpholinobutyrophenone, 4-(dimethylamino)benzophenone, azobisisobutyronitrile, and 2-methyl-4-2-morpholinopropiophenone. Nitrogen atoms commonly exist because they undergo homolytic cleavage upon introducing light energy.[29] For this reason, we assumed that the extracted solution might have nitrogen-containing compounds. In fact, XPS analysis showed that the nitrogen 1 s signal was detected at 400.2 eV (Fig. 3B), indicating that the observed toxicity of the extracted solution might originate from nitrogen-containing photoinitiators.

♦ C. elegans is a unique animal model system with sensing and locomotion abilities

As mentioned in the introduction section, *C. elegans* is able to move away from any positions from which harmful toxic compounds are locally present or released. In contrast, its locomotion direction is not affected in nontoxic environments.[15] The chemotactic properties shown by *C. elegans* can point out a source position from which toxic compounds are released. To this point, the experiments described in Figs. 1–3 demonstrated that photoinitiators and other toxic compounds were released from the 3D cuboids up to a certain toxicity level. Thus, we designed an interesting experiment when fabricating a 3D cuboid. First, a cuboid with the same dimensions ($1 \times 1 \times 0.1$ cm^3) was printed and then was illuminated with UV light for post-curing to minimize the release of toxic compounds. Second, when the post-curing step was carried out, a piece of Al foil was wrapped around one-half of the side of the cuboid (Fig. 4A). We hypothesized that nearly all toxic compounds would be released from the half block without post-UV curing. In fact, the cuboid without post-curing was slightly bent upon applying external force (Fig. 4B).

We observed a particular *C. elegans* worm that closely approached the side of the cuboid without post-curing and then rapidly (< 14 sec) turned away from the cuboid. This 'turn-away' motion might be due to formation of a gradient of toxic compounds released from the cuboids (Fig. 4D, upper photos). This 'turn-away' motion was often found within a 3 mm distance from the edge side of the cuboid. Another case we observed is that the *C. elegans* worm first crossed over the '3 mm' distance approaching the cuboid but then turned away from the cuboid (lower photos).

In contrast to the aforementioned description of the dynamic motion of an individual *C. elegans*, we observed the overall population behavior in a collection. We observed geometrical distributions of all *C. elegans* organisms centered on the cuboid at 1 hr after worm introduction at the designated four points (Fig. 4C). The reason for the 1 hr setting time is to establish the release and gradient formation of toxic substances from the cuboids. We found that *C. elegans* worms were evenly distributed regardless of the

Al foil masked or unmasked regions with a distance range from zero to 10 mm (Fig. 4E, left bars). In other words, nearly 50% of the population of *C. elegans* was found in the masked region, and the remaining 50% was found in the unmasked region. However, when we looked closely at the region from zero to 6 mm, differences in geometrical distributions were found. Approximately 61% of the *C. elegans* worm were crawling in the photocured region, and 39% of the population was found in the masked region (the middle bars) (p-value = 0.0531). This difference in chemotactic behavior was further enhanced when we observed the crawling worms living from zero to 3 mm from the cuboid. Approximately 70% of the *C. elegans* worms were crawling in the photocured region, and 30% of the population was found in the masked region (the right bars) (p-value < 0.001). The results clearly indicate that *C. elegans* can be a unique model organism for detecting toxic compounds because of the combination of locomotion and sensing abilities.

Discussion

Typical model organisms that have been used in the past have contributed a large amount to toxicity assessments of substances. However, typical model organisms are not suitable for determining in which direction chemicals diffuse from leachable materials. We chose 3D-printed products as typical leachable materials. By using a small nematode, *C. elegans*, approximately 1 mm in body length, we were able to carry out a toxicity test that would be difficult to perform with conventional model organisms. The 3D-printed block extract adversely affected the health of *C. elegans*, resulting in reduced lifespan, reduced exercise capacity, reduced number of offspring, and decreased relative expression levels of stress-response genes. In addition, the leaching point and the direction of chemical diffusion could be monitored by following the movement of worms located near the substances. Material toxicity assessments that could not have been conducted with conventional model organisms can be performed by tracking the distribution and behavior of *C. elegans*.

Methods

♦ Materials

A stereo-lithographic 3D printer (Master Plus J) and its resin (Arario 410) containing diglycidyl ether of bisphenol (20–40%), acryloyl morpholine (10–20%), tripropylene glycol diacrylate (20–40%), 1-hydroxycyclohexyl phenyl ketone (3–7%), diphenylphosphine oxide (1–3%), and 2-methyl-4-2-morpholinopropiophenone (1–3%) were purchased from Carima CO, Korea. A dissecting microscope was purchased from Olympus (SZ61, Tokyo, Japan). We printed 3D printed blocks in the same method as in previous studies.[31] The 3D-printed blocks in this study were designed using the commercial 3D modeling program Rhino 3D (Rhinoceros version 5 SR 12, USA). However, any 3D modeling software that generates an .STL format file can be used. The .STL file was sectioned using the StickPlus Rhino 3D plugin, and the data were transmitted to the 3D printer, resulting in a solid product of the 3D model. Except those reported above, all chemical agents were purchased from Sigma-Aldrich CO. St. Louis, MO, USA.

♦ Preparation of 3D-printed blocks, extracts and food sources

3D-printed products were printed in dimensions of 10 mm by 10 mm with a height of 1 mm. The 80 printed blocks and magnetic stirrer were added to 400 mL of Luria-Bertani broth (LB) media, and extraction was carried out for 72 hours at room temperature (Fig. 1A). During the extraction, the bottle was protected from light. Then, the mixture was filtered by a bottle top filter (Sartolab® BT vacuum filter 180C5E, pore size of 0.22 μm). After all the steps mentioned above, *Escherichia coli* OP50 (uracil auxotroph) was grown in 20 ml of extracted LB media at 37°C with shaking (220 rpm) for 16 hours

♦ C. elegans maintenance

The N2 CGCb strain was used as a wild-type control. The CL2070 (hsp-16.2::gfp) and CF1553 (sod-3::gfp) strains were kindly given to us by Sang-Kyu Park (Department of Medical Biotechnology, SoonChunHyang Univ.). Nematode growth medium (NGM) containing 25 mM NaCl, 1.7% agar, 2.5 mg ml^{-1} peptone, 5 μg mL^{-1} cholesterol, 1 mM $CaCl_2$, 1 mM $MgSO_4$, and 50 mM KH_2PO_4 (pH 6.0) was used as a growth medium. All experiments were conducted at 20 °C unless otherwise mentioned. *E. coli* OP50 was added to each NGM plate as a food source.

♦ Lifespan assay

Sixty age-synchronized 3-day-old worms were transferred to fresh NGM plates, and 5-fluoro-2'-deoxyruridine was added to prevent internal hatching. Thereafter, worms were transferred to fresh NGM plates with 5-fluoro-2'-deoxyruridine every other day until all worms were dead. The number of living and dead worms was scored every day. Three independent replicate experiments were performed. Statistical analysis was performed using the log-rank test.[30]

♦ GFP expression of stress-response genes

We applied the method of the previous study to measure the expression of the stress-response gene on the 3D printed block.[32] Age-synchronized CL2070 (hsp-16.2::gfp) and CF1553 (sod-3::gfp) worms were placed in NGM plates supplemented with 3D-printed block extract at 20 °C for 5 days. Then, the worms were mounted on a slide glass coated with 2% agarose and anaesthetized with 1 M sodium azide. After covering the slide with a coverslip, the expression of each reporter gene was observed using a confocal microscope (Nikon FV10i, Nikon, Tokyo, Japan). The fluorescence intensity of a randomly selected single worm was quantified with a fluorescence multiplate reader (Synergy MX, BioTek, Winooski, America).

♦ Fertility assay

In order to measure whether the progeny were affected by the 3D printed block, we applied the method of the previous study.[19] For the fertility assay, five L4/young adult stage worms were transferred to a fresh NGM plate containing 3D-printed block extract and permitted to lay eggs for 5 hrs. The eggs were

maintained at 20 °C for 2 days. A single worm was transferred to a fresh NGM plate containing 3D-printed block extract every day until it laid no eggs. Eggs spawned by a single worm were incubated at 20 °C for 48 hours, and the number of progeny produced was recorded each day. The average number of progeny produced by 5 worms treated with 3D-printed block extract was compared to that produced by control worms.

♦ Body bending assay

This experiment was performed with a slight modification of the previously known *C. elegans* body bending assay.[21] First, this experiment was carried out by using the result of extraction of 3D-printed blocks with double distilled water (DDW) instead of LB. The 8 3D-printed blocks and magnetic stirrers were added to 40 mL of DDW, and extraction was carried out for 72 hours at room temperature (Fig. 2C). During the extraction, the bottle was protected from light. Then, the mixture was filtered by a syringe filter (Satorius Minisart® syringe filter, pore size of 0.2 μm). Upon completion of the extraction, 100 μl of NGM was spread evenly, and OP50 was seeded. After that, we transferred a 3-day-old nematode to the prepared NGM. Before the start of this assay, a worm was put on a sterile fresh NGM agar plate without OP50 and allowed to crawl freely to remove the agglomerated bacteria from the worms (5 days old). After visually examining whether the bacteria were removed, a worm was put into a 96-well plate (SPL 30096, SPL life science CO., Korea) with M9 buffer and allowed to swim freely for 1 min for acclimatization to the environment. Then, the number of thrashes was counted for 1 min. We monitored at least 6 worms for each assay. A worm movement that swings its head and/or tail to the same side is counted as one thrash.

♦ 3D-printed block extract analysis using X-ray photoelectron spectroscopy

The 3D-printed block was extracted with DDW, and 10 μl of the resultant extracted was dropped on a 10 mm by 10 mm Si wafer. Then, the DDW was evaporated naturally. X-ray photoelectron spectroscopy was performed with a Thermo Scientific™ K-Alpha™ X-ray photoelectron spectrometer (XPS) system.

♦ Dead-Zone detection assay

The 3D-printed block was further cured using a piece of aluminum foil, as shown in Fig. 4A, as a photomask covering only half of the block, followed by additional UV irradiation. After that, we put the produced block in the center of the testing plate and put *C. elegans* worms at the same age (3 days old) in four places 20 mm away from the center (Fig. 4C). After incubation at room temperature for 1 hr, we counted the worms that were found within 3 mm, 6 mm and 10 mm from the surface of the block. The following equation was used to quantify the distribution of worms (& are shown in Fig. 4C).

$$\%\ \text{of worms} = \frac{(\#\ \text{of worms in ⓐ or ⓑ})}{(\#\ \text{of worms in ⓐ} + \#\ \text{of worms in ⓑ})} \times 100$$

Declarations

Acknowledgements

This work was supported by a National Research Foundation of Korea (NRF) grant funded by the Korea government (MSIT) (No. 2018R1A5A1025208) and the Disaster and Safety Management Institute (MPSS-CG-2016-02) from The Ministry of Public Safety and Security of the Republic of Korea.

References

1. Thrivikraman, G., Madras, G. & Basu, B. In vitro/in vivo assessment and mechanisms of toxicity of bioceramic materials and its wear particulates. *RSC Advances* **4**, 12763–12781 (2014).
2. Wang, W. Literature review on duckweed toxicity testing. *Environmental Research* **52**, 7–22 (1990).
3. Böcük, H., Yakar, A. & Türker, O. C. Assessment of Lemna gibba L.(duckweed) as a potential ecological indicator for contaminated aquatic ecosystem by boron mine effluent. *Ecological indicators* **29**, 538–548 (2013).
4. 20079, ISO. (International Organization for Standardization, 2005).
5. Khangarot, B., Ray, P. & Chandr, H. Daphnia magna as a model to assess heavy metal toxicity: comparative assessment with mouse system. *Acta hydrochimica et hydrobiologica* **15**, 427–432 (1987).
6. Collard, H.-r. J. *et al.* Toxicity and endocrine disruption in zebrafish (Danio rerio) and two freshwater invertebrates (Daphnia magna and Moina macrocopa) after chronic exposure to mefenamic acid. *Ecotoxicology and environmental safety* **94**, 80–86 (2013).
7. Lele, Z. & Krone, P. The zebrafish as a model system in developmental, toxicological and transgenic research. *Biotechnology advances* **14**, 57–72 (1996).
8. Oskui, S. M. *et al.* Assessing and reducing the toxicity of 3D-printed parts. *Environmental Science & Technology Letters* **3**, 1–6 (2015).
9. Parasuraman, S. Toxicological screening. *Journal of pharmacology & pharmacotherapeutics* **2**, 74 (2011).
10. Morrison, R. J. *et al.* Regulatory considerations in the design and manufacturing of implantable 3D-printed medical devices. *Clinical and translational science* **8**, 594–600 (2015).
11. Kodzius, R., Schulze, F., Gao, X. & Schneider, M. R. (Multidisciplinary Digital Publishing Institute, 2017).

12. Zhu, F., Skommer, J., Friedrich, T., Kaslin, J. & Wlodkowic, D. in *Micro + Nano Materials, Devices, and Systems.* 96680Z (International Society for Optics and Photonics).
13. Karimi, M. Diffusion in polymer solids and solutions. *Mass transfer in chemical engineering processes*, 17–40 (2011).
14. Hernandez, D. D. Factors affecting dimensional precision of consumer 3D printing. *International Journal of Aviation, Aeronautics, and Aerospace* **2**, 2 (2015).
15. Tomioka, M. *et al.* The insulin/PI 3-kinase pathway regulates salt chemotaxis learning in Caenorhabditis elegans. *Neuron* **51**, 613–625 (2006).
16. Hope, I. A. *C. elegans: a practical approach*. Vol. 213 (OUP Oxford, 1999).
17. Hillier, L. W. *et al.* Genomics in C. elegans: so many genes, such a little worm. *Genome research* **15**, 1651–1660 (2005).
18. Strange, K. in *C. elegans* 1–11 (Springer, 2006).
19. Kim, J.-S., Kim, S.-H. & Park, S.-K. Selenocysteine modulates resistance to environmental stress and confers anti-aging effects in C. elegans. *Clinics* **72**, 491–498 (2017).
20. Kim, J.-S. & Park, S.-K. Supplementation of S-ALLYL cysteine improves health span in Caenorhabditis elegans. *Bioscience Journal* **33** (2017).
21. Nawa, M. & Matsuoka, M. The method of the body bending assay using Caenorhabditis elegans. *bio-protocol* **2** (2012).
22. Zhang, L., Jie, G., Zhang, J. & Zhao, B. Significant longevity-extending effects of EGCG on Caenorhabditis elegans under stress. *Free Radical Biology and Medicine* **46**, 414–421 (2009).
23. Leung, M. C. *et al.* Caenorhabditis elegans: an emerging model in biomedical and environmental toxicology. *Toxicological sciences* **106**, 5–28 (2008).
24. Rea, S. L., Wu, D., Cypser, J. R., Vaupel, J. W. & Johnson, T. E. A stress-sensitive reporter predicts longevity in isogenic populations of Caenorhabditis elegans. *Nature genetics* **37**, 894 (2005).
25. Sánchez-Blanco, A. & Kim, S. K. Variable pathogenicity determines individual lifespan in Caenorhabditis elegans. *PLoS genetics* **7**, e1002047 (2011).
26. Stiernagle, T. Maintenance of C. elegans. *C. elegans* **2**, 51–67 (1999).
27. Schafer, W. R. Genetics of egg-laying in worms. *Annu. Rev. Genet.* **40**, 487–509 (2006).
28. Bail, R. *et al.* The effect of a type I photoinitiator on cure kinetics and cell toxicity in projection-microstereolithography. *Procedia CIRP* **5**, 222–225 (2013).
29. Li, Z., Shen, W., Liu, X. & Liu, R. Efficient unimolecular photoinitiators for simultaneous hybrid thiol–yne–epoxy photopolymerization under visible LED light irradiation. *Polymer Chemistry* **8**, 1579–1588 (2017).
30. Peto, R. & Peto, J. Asymptotically efficient rank invariant test procedures. *Journal of the Royal Statistical Society: Series A (General)* **135**, 185–198 (1972).
31. Park, H. K., Shin, M., Kim, B., Park, J. W. & Lee, H. A visible light-curable yet visible wavelength-transparent resin for stereolithography 3D printing. *NPG Asia Materials* **10**, 82–89 (2018).

32. Oh, S.-I., Park, J.-K. & Park, S.-K. Lifespan extension and increased resistance to environmental stressors by N-acetyl-L-cysteine in Caenorhabditis elegans. *Clinics* **70**, 380–386 (2015).

Figures

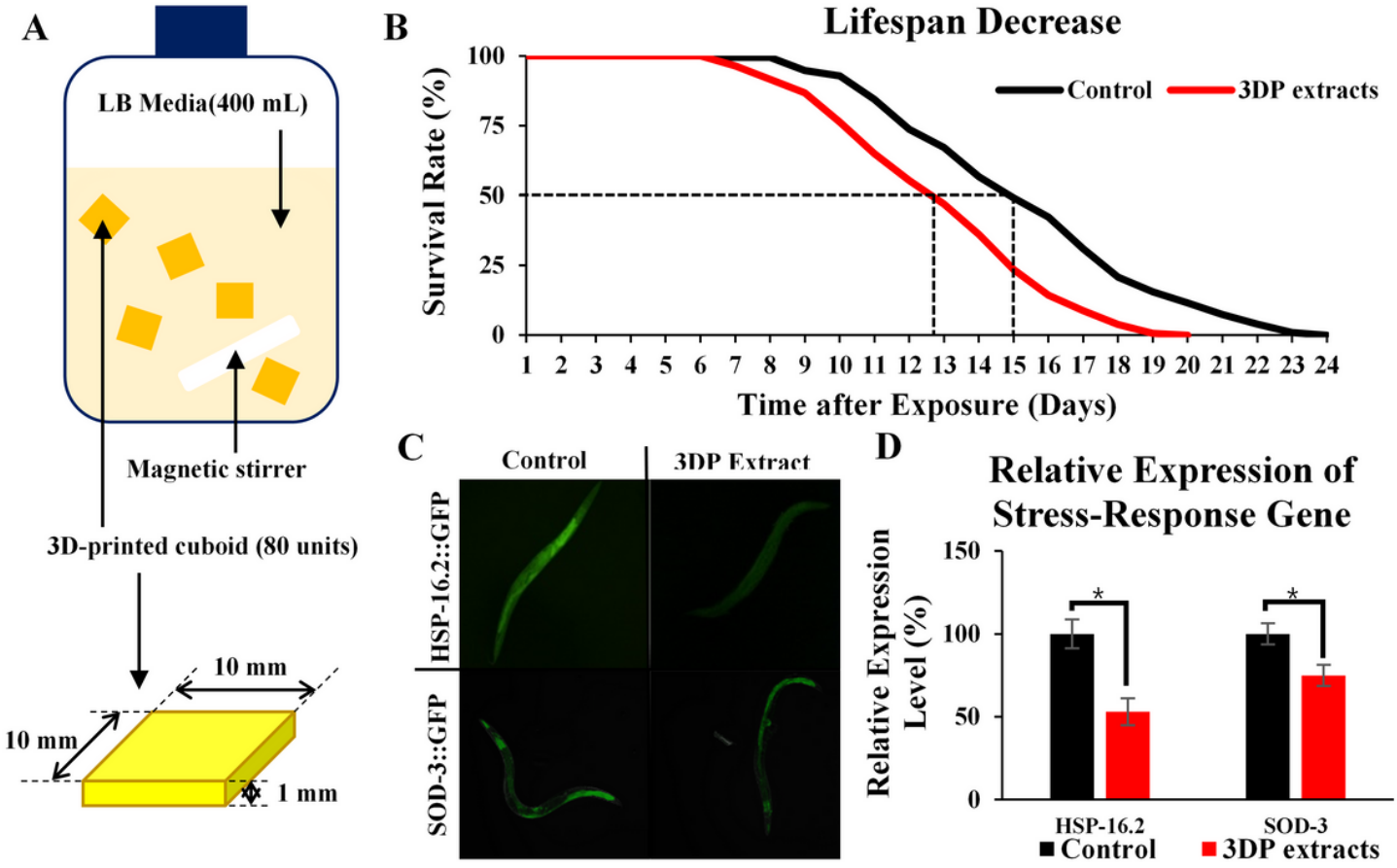

Figure 1

Extraction procedure of 3D-printed cuboids in LB media and the effect of 3D-printed cuboid extracts on C. elegans health. (A) As shown in the scheme, the cuboid was printed in dimensions of 1 x 1 x 0.1 cm3. A total of 80 cuboids and a magnetic stirrer were added to 400 mL of LB media. After the bottle was blocked from light and extracted at room temperature for 72 hours, the following experiments were performed under the corresponding conditions. (B) Lifespan-reducing effect of 3D-printed cuboid extracts. Dotted lines indicate 50% survival of C. elegans. Age-synchronized young adult worms (day 3, n=60) were transferred to NGM plates layered with OP50, which was grown in LB extract, and the number of live/dead worms was recorded every day. Worms that were lost or showed internal hatching during the assay were excluded. The mean lifespan was observed and compared with that of worms grown with OP50 under normal non-toxic conditions, control ($p<0.05$). (C) The stress-response gene expression levels: HSP-16.2::GFP (upper panels) SOD-3::GFP (lower panels). The left column indicates uncontaminated LB supplementation, and the right column is the LB contaminated with released toxic

compounds. (D) Quantitative analysis of the stress-responsive protein expression levels shown in Figure 1C. The black bars are the results obtained using uncontaminated LB supplementation, and the red bars are the results obtained using the LB contaminated with released toxic compounds. The asterisks indicate p-values less than 0.05 compared with the control.

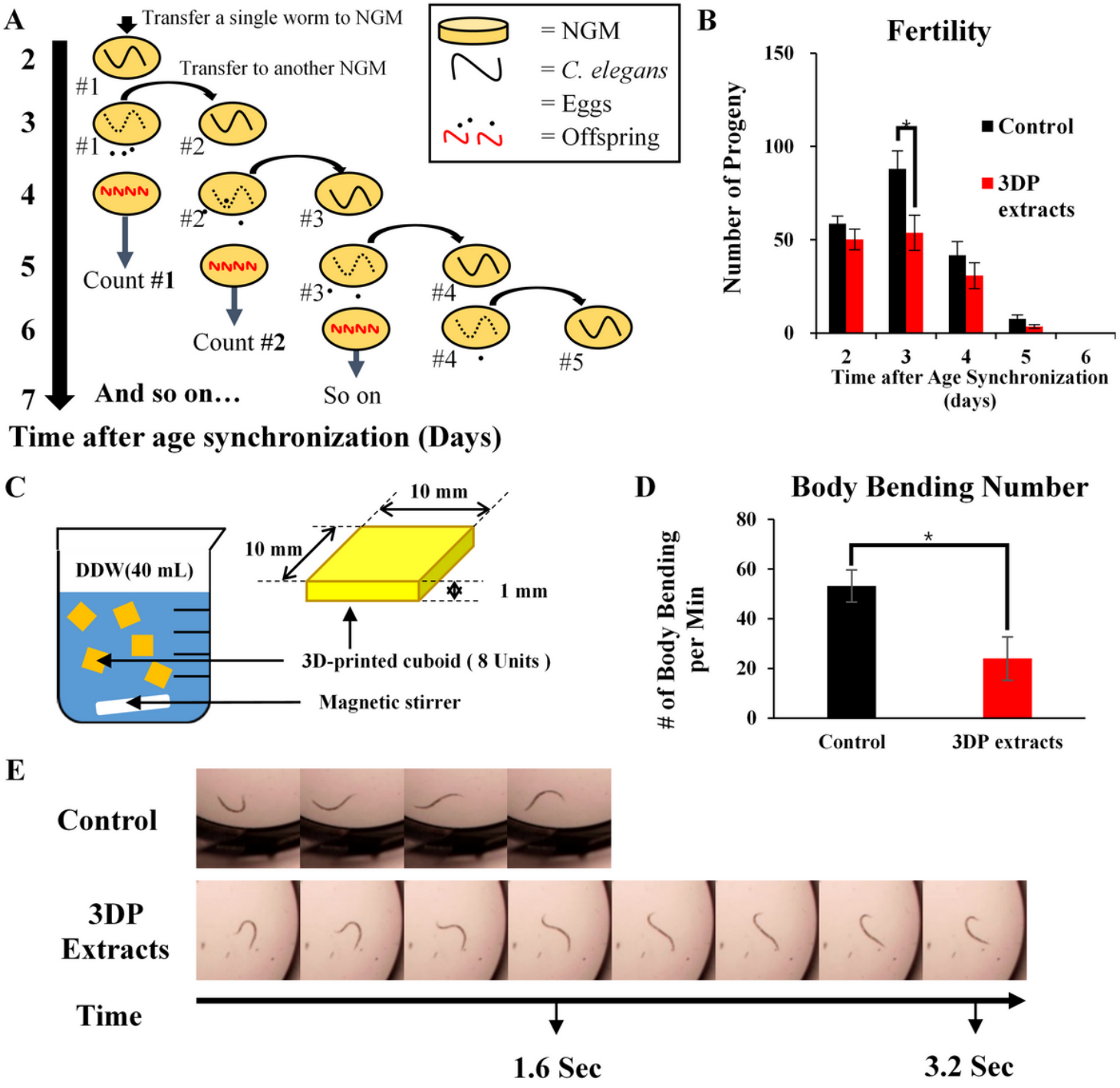

Figure 2

Extraction procedure of 3D-printed cuboids in DDW and mobility decreases. (A) Schematic procedure for the fertility assay of C. elegans. (B) 3D-printed object extracts decrease fertility on day 3. The number of progeny produced was monitored every day during a gravid period. Data show the mean number of

progeny produced by 5 individual worms on each day. Asterisks indicate p-values less than 0.05 compared with the control. (C) Extraction procedure of 3D-printed blocks in DDW (previously LB media). After a 72 hr extraction step, the extract was filtered through a 0.2 μm pore syringe filter. (D) Total number of body bends in 1 minute. The control (black) bent 53.16 times per minute, while worms exposed to 3D-printed cuboid extract (red) bent 24 times per minute (n=6). Asterisks indicate p-values less than 0.05 compared with the control, and the error bar indicates standard error. (E) Representative time-lapse photo arrays of body bending. Compared to the control worm, the worm treated with the 3D-printed cuboid extract took twice as much time to turn in the opposite direction.

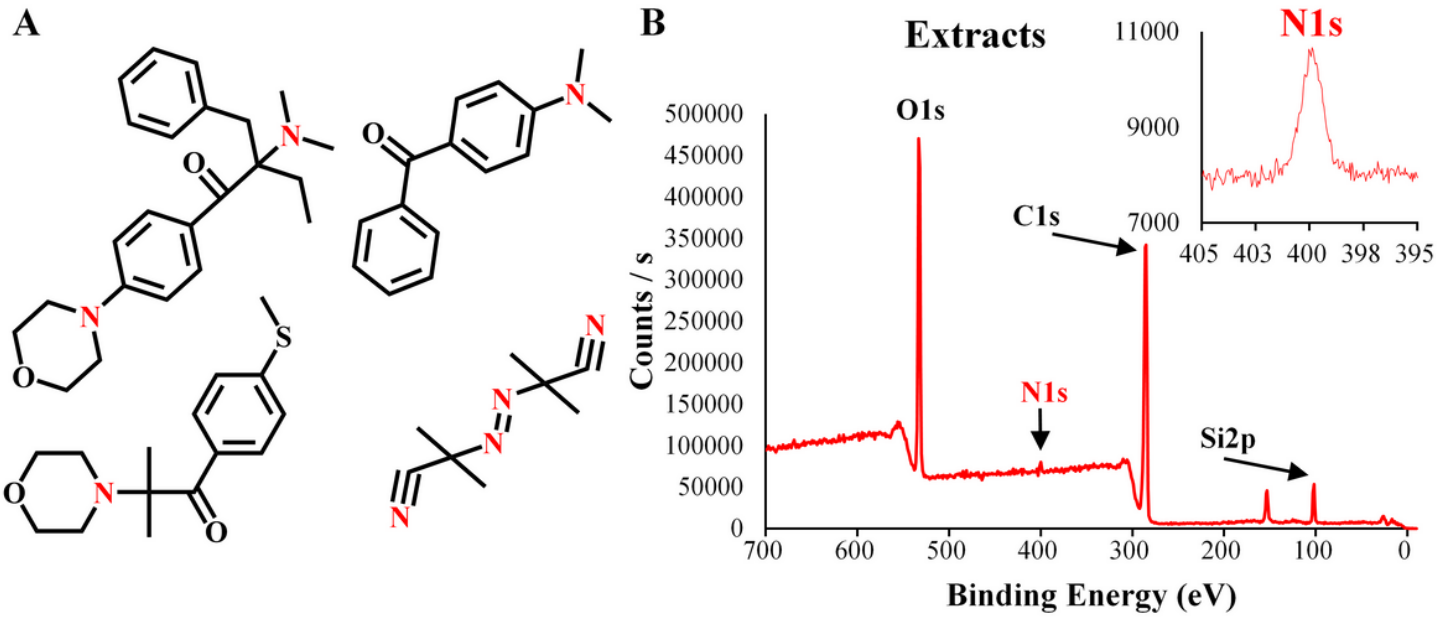

Figure 3

Commonly used photoinitiators and XPS data of 3D-printed cuboid extracts. (A) Chemical structures of commonly used photoinitiators. Clockwise from the top-left, 2-benzyl-2-(dimethylamino)-4'-morpholinobutyrophenone, 4-(dimethylamino)benzophenone, azobisisobutyronitrile, and 2-methyl-4-2-morpholinopropiophenone. Amine groups are marked in red. (B) XPS data of 3D-printed cuboid extracts. The inset plot is an enlargement of the N1s peak. XPS analysis showed the presence of nitrogen.

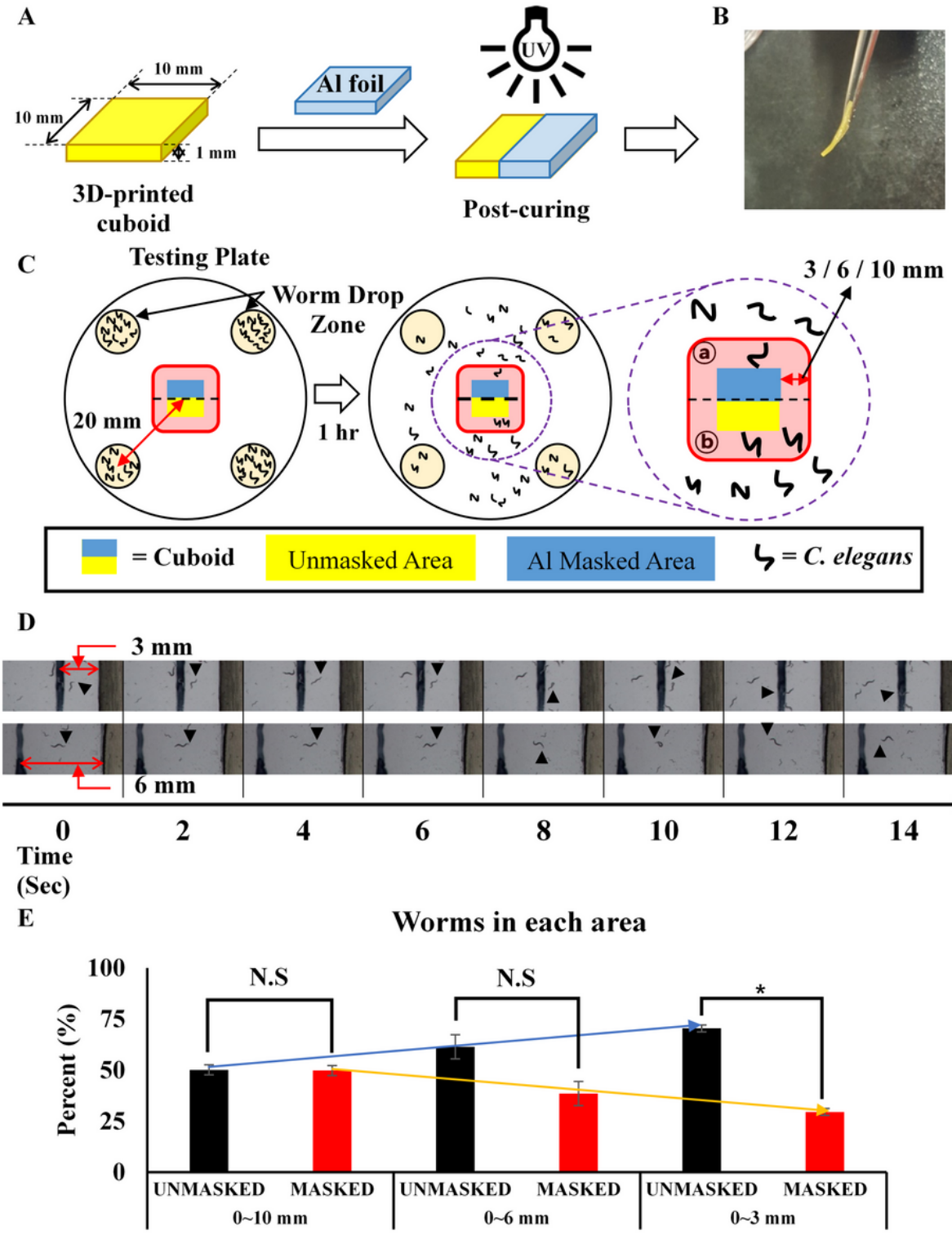

Figure 4

Half area-cured 3D-printed material monitored in the presence of C. elegans. (A) Scheme of additional curing of a 3D-printed cuboid. Half of the cuboid is wrapped with aluminum foil (used as photomask, blue), and then additional curing is performed using a UV curing machine for 1 minute. (B) Picture of the result of additional UV curing of a 3D-printed cuboid. The area that was masked by Al foil was relatively softer than the area that was not. (C) Design of the testing plate for an additionally photocured area

detection assay using C. elegans. The apricot color is the ‘worm drop zone’, which indicates where C. elegans worms are placed at the beginning of the experiment. We tested whether the worms could distinguish between two areas, the additionally masked area and the unmasked area. The object resulting from the procedure in (A) was placed at the center of the testing plate, and the worm drop was placed 20 mm from the center. After placing the worm drop, the worms were incubated at room temperature for 1 hr. Then, the number of worms in the designated area was counted. (D) Representative time-lapse photo arrays of locomotion. The top shows the area 3 mm away from the 3D-printed cuboid, and the bottom is the area 6 mm away from the cuboid. (E) Result of the additionally photocured area detection assay using C. elegans. Regarding the middle bars, which include worms in the area within 0 to 6 mm, 61.42% of the worms were in the unmasked area, and 38.57% of the population was in the masked area (p-value = 0.0531). Regarding the right bars, which include the worms in the 0-3 mm area, there were 70.45% of the worms in the unmasked area and 29.54% in the masked area (p-value < 0.001). Colored arrows (blue, yellow) are marked to show trends. Asterisks indicate p-values less than 0.05 compared with the control, and the error bar indicates standard error.